

Polar ozone depletion: A three-dimensional chemical modeling study of its long-term global impact

Richard S. Eckman, William L. Grose, Richard E. Turner, and W. Thomas Blackshear
NASA Langley Research Center, Hampton, Virginia

Abstract

The export of ozone-poor air from the polar region following the breakup of the southern hemisphere polar vortex is examined with a three-dimensional chemistry transport model. This volume of depleted ozone, the result of chemical processing during the southern wintertime and springtime, is long-lived in the lower stratosphere and can affect ozone concentrations at southern middle latitudes following its transport out of the polar region. Two 5-year simulations were performed utilizing the NASA Langley Research Center three-dimensional chemistry transport model. One simulation included only gas phase and sulfate aerosol chemistry, while the second simulation also included reactions occurring on polar stratospheric clouds (PSCs). The model-calculated seasonal variation of southern hemispheric O_3 , HNO_3 , and active chlorine as a result of PSC chemistry is in reasonable accord with satellite observations. The model reveals that ozone is transported equatorward following the breakup of the polar vortex to approximately $20^\circ S$ latitude by the first southern summer following the activation of PSC chemistry. A residual column-integrated ozone depletion of 9% remained by the springtime of the second year. In subsequent years, the southern ozone hole itself increased in depth from a column-integrated depletion of 37% in the first year to 43% in the fifth year with respect to the baseline simulation with no PSC chemistry. The isopleths of column-integrated ozone loss showed a slow equatorward movement during the 5-year run. These model results, in general agreement with earlier model studies using parameterized chemistry, show that a potential exists for a long-term accumulation of ozone loss in the southern polar region and a gradual increase in the global impact of polar ozone depletion. Comparison with satellite and ground-based observations of ozone trends at midlatitudes suggests that ozone dilution may be a contributing factor. Experiments were performed to examine the sensitivity of the rate of local ozone recovery following the breakup of the vortex to the depth and spatial extent of the denitrification of polar air. These simulations revealed that deeper denitrification led to a more persistent column-integrated ozone loss and a slight increase in its equatorward progression.

Introduction

Observed downward trends in stratospheric ozone at midlatitudes during the last 15 years remain poorly understood [e.g., *World Meteorological Organization (WMO)*, 1995]. Several possible explanations (which are not necessarily mutually exclusive) for these trends have been proposed. *Hofmann and Solomon* [1989] suggested that heterogeneous chemical reactions on sulfate aerosols might contribute substantially to midlatitude ozone destruction. Observations of changes in ozone and key nitrogen species (NO_2 and HNO_3) that occurred after the Mount Pinatubo volcanic eruption in 1991 lend credence to this theory [e.g., *Fahey et al.*, 1993; *Hofmann et al.*, 1994a; *Hofmann et al.*, 1994b; *Rinsland et al.*, 1994]. In a recent paper, *Solomon et al.* [1996], using a two-dimensional model [*Garcia et al.*, 1992; *Garcia and Solomon*, 1994] with time-varying aerosol burden as an input parameter, conclude that the aerosols enhance ozone depletion at northern midlatitudes. The results from this study show substantial success in modeling the temporal evolution and trend in the midlatitude, northern hemisphere ozone, even though the calculated columnar changes are smaller (approximately 50%) than indicated by the total ozone mapping spectrometer (TOMS) O_3 data. However, other studies [e.g., *Bojkov*, 1993; *Chandra*, 1993] have argued that these observed changes may not necessarily be a consequence of increased sulfate aerosol burden following the volcanic eruption.

An alternate explanation suggested that downward trends in midlatitude ozone might be a consequence of polar vortex processing [e.g., *Tuck*, 1989; *Tuck*, 1992] with subsequent transport to midlatitudes of air masses having enhanced levels of reactive chlorine and depressed levels of active nitrogen. A study conducted with a three-dimensional chemistry transport model with horizontal resolution of 2.5 degrees in longitude and 2 degrees in latitude and using a simplified formulation for reactive chlorine [*Douglass et al.*, 1991; *Kaye et al.*, 1991] indicated that the effect is too small to explain the observed midlatitude northern hemisphere ozone loss. Studies of vortex erosion and filamentation [e.g., *Waugh et al.*, 1994] also suggest that this processing may not be as large as suggested by A. F. Tuck. Further work needs to be done to better quantify the magnitude of this effect.

Another explanation that relates ozone trends to polar ozone depletion is the so-called "dilution effect" [e.g., *Chipperfield and Pyle*, 1988; *Sze*, 1989; *Grose et al.*, 1990; *Prather et al.*, 1990; *Cariolle et al.*, 1990]. The dilution effect is especially appealing for the southern hemisphere because of the much larger and more pervasive po-

lar ozone destruction occurring during springtime in the Antarctic region relative to that occurring in the Arctic region. Dilution of the midlatitude air occurs as a result of export of ozone-poor air by quasi-horizontal transport following the breakup of the southern polar vortex during the seasonal transition in the stratosphere. This dilution could create a deficit in ozone which might persist for a lengthy period because of the long chemical lifetime of odd oxygen in the lower stratosphere [*Brasseur and Solomon*, 1984]. If the deficit persists until the next Antarctic spring, the effect might be cumulative and have consequences for the global ozone budget. *Atkinson et al.* [1989] concluded that anomalously low total ozone values observed over Australia and New Zealand during December 1987 were the result of ozone-poor air from the polar region being transported toward midlatitudes. Evidence for this large-scale latitudinal mass exchange can be seen in their potential vorticity analyses and the strong correlation with the evolution of total ozone from TOMS data.

Three-dimensional studies of ozone dilution with varying degrees of complexity have been performed by several groups. *Cariolle et al.* [1990] introduced an ozone loss consistent with 1987 Antarctic ozone hole conditions into a three-dimensional general circulation model (GCM). The model employed linearized ozone photochemistry, but allowed the calculated ozone to interact radiatively with the general circulation model. An 11-month model integration revealed a residual ozone destruction in the southern hemisphere summer of 0.8% with the midlatitude spread limited to a region between 390 and 470 K (approximately 100 hPa to 35 hPa). *Grose et al.* [1990] performed a similar study with a three-dimensional GCM/CTM with a complete gas phase chemistry scheme run in an off-line manner. An ozone loss was imposed on the model consistent with the latitudinal and vertical extent of observed southern polar ozone depletion. One year following the imposition of the ozone hole, a small, but significant, residual deficit in southern hemispheric column ozone of approximately 1% was calculated. *Prather et al.* [1990], using a three-dimensional CTM with linearized ozone photochemistry, performed a multiyear integration with an imposed ozone hole and examined its dynamical dilution. After 1 year, the calculated residual ozone deficit was 2% at latitudes as far north as 40°S. With the hole reimposed 1 year later, the cumulative decrease during the second year was 20% more than at the end of the first year.

More recently, *Mahlman et al.* [1994] examined the problem using the Geophysical Fluid Dynamics Laboratory (GFDL) SKIHI GCM. An ozone hole was imposed and allowed to recover using parameterized chemistry.

The 4.5-year simulation compared to a control experiment showed a long-term accumulation of ozone loss as ozone reductions (greater than 2% poleward of 30°S) remained at the beginning of subsequent southern winters. They suggested that the potential exists for a positive temperature-chemical feedback as the lowered ozone levels led to progressively colder temperatures and the potential for enhanced ice cloud formation.

Until recently, multiyear simulations of the three-dimensional evolution of the middle atmosphere with a GCM having a reasonably complete representation of both gas phase and heterogeneous chemistry have required prohibitively large amounts of computational time. The present study differs from previous three-dimensional modeling studies of ozone dilution in that it uses a comprehensive stratospheric gas phase chemistry scheme as well as simple, but reasonable, parameterizations for chemistry occurring on both polar stratospheric clouds and sulfate aerosols. Previous three-dimensional studies have used either linearized ozone chemistry or have imposed ozone holes representative of observed conditions. We use the NASA Langley three-dimensional general circulation model (GCM) and chemistry transport model (CTM) to investigate the possible impact of ozone dilution on the global ozone budget.

The paper is organized as follows: The following section describes the three-dimensional model and the multiyear simulations which were performed. The results of these experiments are then presented and contrasted with those of other investigations and with observations. In the final section, we summarize the results and outline plans for some related experiments.

Experiment Description

The NASA Langley Research Center three-dimensional GCM and chemistry transport model (CTM) are used in this study. *Eckman et al.* [1995] recently presented a full description of the CTM and discussed its performance in simulating Antarctic ozone depletion compared with observations. The model used in the present study is essentially identical to the one used in the above work. Briefly, the GCM is global in extent and uses a spectral representation of the dependent variables in the horizontal dimension with triangular truncation (zonal wavenumber 16 (T16), in the version employed for this study). The model vertical domain spans the surface to approximately 60 km in 24 levels. There are 14 levels above the tropopause with a vertical resolution of approximately 3 km. Fifteen chemical families of individual constituents are explicitly transported. They are odd oxygen ($O_x = O + O(^1D) + O_3$), total

odd nitrogen ($NO_y = N + NO + NO_2 + NO_3 + 2N_2O_5 + HNO_3 + HO_2NO_2 + ClONO_2$), HNO_3 , total inorganic chlorine ($Cl_y = Cl + ClO + HOCl + HCl + ClONO_2 + 2Cl_2 + 2Cl_2O_2$), N_2O_5 , H_2O_2 , HCl , $ClONO_2$, N_2O , $CFCl_3$, CF_2Cl_2 , CCl_4 , CH_3Cl , CH_3CCl_3 , and a proxy for condensed phase nitric acid. Bromine chemistry is not included in the present simulation, which partially accounts for a smaller calculated southern polar ozone depletion than observed. An “off-line” transport approach is employed. The winds and temperatures calculated by the general circulation model are used as inputs to the CTM in the calculation of chemical sources and sinks and the advection of the constituents. There is no feedback between the CTM-calculated ozone and the GCM radiative algorithm in this version of the model. We use annually repeating wind and temperature fields for the multiyear simulation. This removes any possible ozone response due to interannual variability and simplifies the interpretation of the trend results.

As discussed by *Eckman et al.* [1995], the breakup of the model southern polar vortex is slower and more radiatively controlled than indicated by observations. The weaker dynamical activity in the model during the vortex breakup period results in the export of ozone-poor air to midlatitudes taking place more slowly. However, the relevant timescale for ozone dilution is the ozone replacement time in the lower stratosphere which is on the order of months to a year, depending on latitude [e.g., *WMO*, 1989]. To better characterize the export of air from the vortex, we have run an experiment with the CTM in which a tracer was initialized in the southern vortex region during July and followed for 1.5 years. By December of the first year, the tracer had already dispersed to approximately 30°S. The export of material well into midlatitudes within 2 months of the maximum ozone depletion confirms that the export of material from the vortex proceeds much more rapidly than the ozone replacement time in the CTM.

We performed a 5-year baseline simulation which includes both gas phase chemistry and reactions occurring on background sulfate aerosols. The sulfate distribution is taken from *WMO* [1992] and we use values 2 times the minimum levels which are representative of the late 1980s [e.g., *Garcia and Solomon*, 1994]. Three additional multiyear runs were made using the same GCM flow fields and initial chemical conditions, but including a parameterization of the reactions occurring on polar stratospheric clouds (PSCs). Different formulations for denitrification were used in each run. In case A, the denitrification is identical to that described by *Eckman et al.* [1995] where nitrogen is removed with a 5-day time constant when temperatures fall below the PSC type II threshold temperature

of 186 K. When temperatures are above this level but below the type I threshold, a weak denitrification with a 30-day time constant is imposed, similar to the scheme employed by *Granier and Brasseur* [1992]. A second simulation, case B, differed from case A in that denitrification occurs only when the GCM-calculated temperatures fall less than 186 K and uses a removal time constant of 30 days, in line with particle fallout times given by *Turco et al.* [1989]. This leads to a more physically realistic removal of odd nitrogen compared with case A. To explore this sensitivity further, a third integration, case C, was performed where no irreversible denitrification was allowed to occur; odd nitrogen was returned to active forms when temperatures rose above the PSC type I threshold temperature. Interannual variability in stratospheric temperature [e.g., *WMO*, 1995] can lead to varying levels of denitrification in the southern polar region. While these model simulations employ cyclically repeating temperatures and thus have no interannual temperature variability, these sensitivity studies provide some bounds on the impact of denitrification on ozone loss and its subsequent export to lower latitudes. The model presently does not include a mechanism for dehydration, known to be important in the southern polar stratosphere [e.g., *Kelly et al.*, 1989] as H₂O is not explicitly calculated.

The surface mixing ratios of the chlorine source gases (e.g., F11 and F12) are fixed to levels recommended by *WMO* [1992] which are appropriate to 1990 conditions. The use of constant values in the model removes any increase in ozone depletion due to the observed growth of the chlorine source gases during the 1980s [e.g., *WMO*, 1995]. Similarly, the solar ultraviolet irradiance was held constant during the 5-year simulation. Therefore, no solar cycle-induced component to the interannual ozone trend is introduced into the calculation. These steps were taken to isolate further the impact of transport and chemical processes resulting from PSC-induced ozone depletion during the multiyear simulation.

Results and Discussion

There is considerable observational evidence for the reduction of stratospheric ozone at midlatitudes during the last 15 years [e.g., *WMO*, 1995]. *Stolarski et al.* [1991] derived trends in total ozone from the total ozone mapping spectrometer (TOMS) instrument and found them significant poleward of 20° in both hemispheres. Further analysis of TOMS data yields total ozone trends with values of about 3–5%/decade at midlatitudes in both hemispheres [*WMO*, 1995]. Figure 1 (adapted from *WMO* [1995], Figure 1-7) shows trends derived from measurements by

the Nimbus 7 solar backscatter ultraviolet spectrometer (SBUV) and the ground-based Dobson spectrometer network which are in good accord with the TOMS results, at least prior to the eruption of Mount Pinatubo in 1991.

Measurements by the stratospheric aerosol and gas experiment (SAGE) I and SAGE II instruments show that the ozone loss occurs primarily below 20 km at midlatitudes [*McCormick et al.*, 1992], although there are differences in the magnitude of the SAGE-derived column-integrated ozone trend when compared with ozonesondes and other space-borne instruments [*WMO*, 1995]. In the 25–30 km range neither satellite nor ground-based instruments measure statistically significant trends during the 1980s [*WMO*, 1995].

Trace Gas Seasonal Evolution

Plate 1 shows model results of the temporal evolution of column-integrated ozone on 4 days separated by approximately 3 months during the second and third years of the simulation for case B employing an orthographic projection centered at 60°S latitude and 105°W longitude to highlight southern hemisphere polar processes. By April, column ozone levels have recovered from the previous year's minimum of approximately 145 Dobson Units (DU). Some ozone depletion is evident in July, due to a combination of both PSC and sulfate aerosol processing. The collar region of high column ozone surrounding the pole increases throughout polar winter and maximizes in southern polar springtime, consistent with TOMS total ozone observations [*Newman et al.*, 1993]. Maximum ozone depletion is seen in mid-October followed by a gradual recovery during the later spring period. By the following January (year 3), column-integrated ozone values have substantially recovered in the area around Antarctica, but the collar region of high ozone surrounding the pole is at much reduced levels due, in part, to the normal seasonal decrease of this region during the austral summer. For this time period, the collar region is stronger in the baseline simulation (not shown). This suggests that the impact of the dilution of ozone-poor air to lower latitudes is also a factor in the reduced strength of the collar region in the case B simulation.

Vertical profiles of the modeled percentage difference of zonally averaged ozone between the baseline simulation and case B for each season are shown in Figure 2. The solid lines (years 2 and 3) in each panel correspond to the ozone column sums presented in Plate 1, while the dotted lines (years 1 and 2) are for the same day in the preceding year. Positive percentage differences represent ozone loss resulting from PSC-catalyzed destruction.

During the first year, a small ozone decrease is noted

in midwinter. By October, the majority of ozone depletion occurs in the lower stratosphere below 30 hPa. The level of maximum reduction in the model is somewhat higher than observed in the atmosphere and is due to the model's cold midstratospheric polar temperatures triggering PSC formation at somewhat higher altitudes than observed.

Following the breakup of the Antarctic vortex, additional transport of ozone-poor air toward midlatitudes occurs, resulting in enhanced depletion at midlatitudes in January with a local depletion of 12.6% at 36°S during the second year (dotted line). Ozone reductions are maintained in the lower stratosphere throughout the following model year. In July of the second year, ozone levels are 9.5% less than the baseline run (which includes no PSC chemistry). Calculated ozone depletion in the lower stratosphere is 10.5% at 36°S latitude in October of year 2, a carryover from the previous year's springtime depletion and subsequent dilution to midlatitudes.

The vertical profiles also show that a significant amount of the ozone depletion resides below the 100-hPa level at midlatitudes. This result is in agreement with the work of *Prather et al.* [1990] who see a gradual mixing of ozone-poor air into the upper troposphere. Little chemical ozone destruction occurs below the 128-hPa level in the Langley 3-D model as heterogeneous chemistry is restricted to the region above this level [*Eckman et al.*, 1993]. In addition, the location of the modeled midlatitude ozone reduction is in reasonable agreement with measurements which show maximum reductions at midlatitudes in the 15-20 km region (approximately 120-50 hPa) [*WMO*, 1995]. The modeled ozone reduction becomes insignificant at altitudes higher than 25 km, again in accord with observations.

Model HNO₃ at 45 hPa is presented in Plate 2 for April, July, and October of year 2 and January of year 3 of the case B simulation. By southern autumn, HNO₃ levels have recovered significantly from denitrification during the previous spring. In contrast, by October, a majority of the HNO₃ is removed from the atmosphere, consistent with Upper Atmosphere Research Satellite (UARS) cryogenic limb array etalon spectrometer (CLAES) [*Roche et al.*, 1994] and microwave limb sounder (MLS) observations [*Santee et al.*, 1995]. During January, recovery is proceeding, but levels of HNO₃ are still approximately 3 ppbv lower in the polar region compared with the baseline simulation where PSC chemistry is not enabled.

Figure 3 shows vertical profiles of the HNO₃ mixing ratio during the second through third years of the simulation corresponding to Plate 2. The region of significant denitrification, as represented by a depletion in HNO₃, occurs at substantially the same altitudes as the ozone de-

creases shown in Figure 2. At midlatitudes (36°S), levels of HNO₃ are much smaller than at high latitudes and the reduction in HNO₃ is small as a result of transport of HNO₃-poor air, reaching a maximum in a narrow region near 30 hPa in January and April.

Active chlorine (Cl + ClO + HOCl + 2Cl₂O₂) levels at 45 hPa for the July and October are shown in Plate 3. During the summer and autumn, levels of active chlorine are very low. Active chlorine reaches levels of approximately 2 ppbv during July, decreasing to about 1.3 ppbv in October over a much reduced region of the southern polar region in reasonable accord with MLS ClO observations [e.g., *Waters et al.*, 1993; *Santee et al.*, 1995].

Column Ozone Response

Plate 4 shows the column ozone results of the 5-year simulation. The percent difference in column-integrated, zonally averaged ozone between the simulations with and without chemistry occurring on PSCs is plotted as a function of latitude and time. We use case B, described above, as the simulation employing PSC chemistry. Negative numbers represent a depletion of ozone with respect to the baseline (no PSC) run. The formation and subsequent recovery of southern polar ozone during the southern late winter and spring seasons is evident. The depth of the maximum ozone depletion increases with succeeding years of the simulation with levels ranging from 37% during the first year to 43% in the fifth year. Column ozone recovers during southern summer and autumn, but a column ozone depletion of greater than 10% remains before the onset of the next ozone depletion cycle. The dilution of ozone-poor air from the polar region to midlatitudes progresses during the entire 5-year period with 1–2% ozone depletions reaching 20°S latitude by the second model year. A slow equatorward progression of the depletion isopleths is seen. In the tropics, there is only a very small (less than 1%) ozone reduction.

Comparison with our earlier three-dimensional model dilution experiment [*Grose et al.*, 1990] reveals that the global impact on ozone is now larger and more persistent. That experiment artificially imposed an ozone loss consistent with observations only during the month of September and did not perturb any of the model's other chemical species. PSC-induced ozone loss could not occur at other times or outside of a prescribed area at high southern latitudes. In the current version of the model, temperatures consistent with PSC formation occur at latitudes farther equatorward.

In the northern hemisphere, some ozone depletion is calculated, although the levels are greater than those typically observed during recent northern winter and spring

seasons. As noted by *Eckman et al.* [1995] the model cold-pole bias, a feature common to many general circulation models, triggers heterogeneous chemistry at levels in excess of those observed in the atmosphere. The slow equatorward progression of ozone-poor air in the north mirrors the southern hemispheric situation, albeit at much reduced levels. Similarly, the maximum column ozone depletion in the northern hemisphere grows slowly during the 5-year model run.

Comparison with TOMS satellite and ground-based measurements (see Figure 1) reveal areas of agreement and disagreement with the model. While observations show significant ozone reductions at midlatitudes in both hemispheres of roughly equal magnitude, the model calculates significantly more ozone reduction in the southern hemisphere as a result of the export of ozone-poor air from the polar region. It is, therefore, unlikely that ozone dilution, alone, can account for observed decadal trends in total ozone. The model results also show that ozone dilution is not a source of a significant ozone trend in the tropics, in accord with the absence of statistically significant measured trends in this region [e.g., *WMO*, 1995]

The model-calculated ozone results were globally integrated to examine the long-term stability of the baseline simulation. In Figure 4a, the global ozone sum in Dobson Units is shown for the 5-year period for both the baseline (no PSC) and case B simulations. The baseline simulation shows less than 0.15% decrease over the 5-year period, measured at the annual peak occurring in springtime. In contrast, the simulation with PSC chemistry shows a marked decline during the period. This gives us confidence that the derived ozone differences presented in Plate 4 are due only to PSC-induced changes in ozone.

The impact of ozone dilution on the global ozone budget is presented in Figure 4b. The maximum globally integrated depletion in the first year of the model simulation is 3.6% and rises during the remaining 4 years of the simulation to 5.8%. The rate of increase of the integrated ozone deficit is not linear, but appears to be reaching an asymptotic limit during the final years of the simulation. It is difficult to extrapolate this five-year result to make comparisons with the observed decadal trends presented in Figure 1. The percentage difference shown in Plate 4 represents the level of ozone deficit with respect to a simulation without chemistry occurring on polar stratospheric clouds. This is an idealized result compared with the observed trends reported during the 1980s which are with respect to conditions where polar processes have been occurring in a persistent seasonal manner. The model results suggest that the dilution of ozone-poor air may be a plausible contributing factor to the observed downward trends

in midlatitude ozone during the 1980s.

The majority of the ozone change takes place in the southern hemisphere. Figure 5a shows that the maximum integrated ozone depletion in the southern hemisphere is 10.6% during the simulation occurring with the same phase as the global ozone deficit. In the northern hemisphere, Figure 5b shows that the change is relatively small with a maximum ozone deficit of 2.5% with maximum depletion during northern spring, roughly 180 degrees out of phase with the global and southern hemispheric response.

Sensitivity Studies

To test the sensitivity of the residual ozone depletion to the effects of denitrification and sulfate loading several additional scenarios were run. In case A, presented in Plate 5, the residual southern hemispheric ozone depletion found during the summer is larger than in case B. Case A yields much higher levels of denitrification than the other cases run. Levels of HNO_3 and N_2O_5 remain depressed in the southern polar region throughout the summer and autumn and do not approach the levels of recovery seen in case B where a more physically based parameterization is employed. Little change, however, is seen in the annual deepening of the southern ozone hole in October between the two cases.

Levels of HNO_3 exhibit a continuous year-to-year loss in both cases A and B. Figure 6 shows the zonally averaged model HNO_3 at 80°S in January for each year of the simulation for case B. This loss of HNO_3 is most rapid during the first 3 years of the simulation and lessens in later years. The annual decrease in HNO_3 is greater for case A which has a more rapid denitrification rate (not shown).

An additional case with no irreversible denitrification, case C, was run to test its impact on ozone depletion. In this instance, while HNO_3 was allowed to convert into the condensed phase, it was not subject to sedimentation. As expected, there is no change in HNO_3 from year to year. Case C yields ozone depletion and recovery results which are very similar to case B. The depth of the Antarctic ozone hole is nearly identical to that of case B. However, the equatorward progression of ozone dilution is slightly less rapid in case C with the 0.5% ozone decrease isopleth located about 5° farther south after two model years when compared to the case B result shown in Plate 4.

Prather and Jaffe [1990] showed that the export of air parcels containing denitrified air sustained higher levels of ClO which could have a local impact on the chemistry at midlatitudes. If this air is already substantially depleted of ozone, small increases in ozone are possible as a re-

sult of the reduction in NO_x -catalyzed loss. While our model results reveal substantial reductions in active nitrogen abundances in case B compared to the case C (where no denitrification is allowed to occur) and an increase in active chlorine, there is only a very small difference (less than 0.3%) in the resultant depth of the ozone hole at mid-latitudes. The lack of bromine chemistry in this version of the model may inhibit our ability to accurately model the impact of this chemical propagation.

These sensitivity studies reveal that the model calculation of the depth of the Antarctic polar ozone hole is relatively insensitive to the level of denitrification. Ozone loss due to type II PSC processes dominates that due to type I PSCs as a result of the model's cold-pole bias. The three model cases do reveal that the equatorward progression of ozone loss is very weakly dependent on the rate of denitrification.

Two additional 1-year runs were performed which are identical to the baseline and PSC (case B) scenarios already described, but without background sulfate chemistry enabled. The difference in column-integrated ozone depletion in this instance was very similar to that presented in Plate 4. There was somewhat less ozone depletion in the northern hemisphere, but the latitudinal and temporal morphology of the ozone decreases in the southern hemisphere was nearly identical to the case with background aerosol chemistry included.

Conclusions

A three-dimensional chemistry transport model simulation of the long-term impact of ozone depletion on the global ozone budget has been performed. The model exhibits an annual austral springtime, high-latitude ozone depletion in reasonable accord with observations. Other trace species, such as ClO and HNO_3 show similar responses when compared to UARS observations. The equatorward transport of ozone following the breakup of the polar vortex reaches latitudes as far north as 20°S by the first austral summer following the initiation of the experiment. The year-to-year buildup of the depth of the ozone hole is small, with an additional 6% contribution to the depletion after the fifth model year. These results are in general agreement with earlier experiments performed by *Cariolle et al.* [1990], *Prather et al.* [1990], *Grose et al.* [1990], and *Mahlman et al.* [1994]. Despite considerably different model formulations, a long-term, equatorward transport of ozone-poor air is calculated in all cases. The level of residual ozone depletion and the rate of equatorward progression of ozone-poor air differs in detail depending on the model considered.

Globally and hemispherically integrated ozone differences between the simulations with and without chemical processes occurring on PSCs suggest that ozone dilution can be a factor in explaining the observed downward decadal trends in midlatitude ozone. However, our results show significantly larger ozone reductions at southern midlatitudes compared with the northern hemisphere in accord with the modeling studies of *Mahlman et al.* [1994]. As measurements show comparable decadal ozone reductions at midlatitudes in both hemispheres, it is unlikely that ozone dilution can be the sole factor driving such trends. As mentioned in the introduction, in situ processes occurring on aerosols [e.g., *Solomon et al.*, 1996] may also be a factor in explaining observed trends, at least at northern midlatitudes.

These results must be qualified as other factors such as solar variability, increasing stratospheric chlorine [e.g., *Jiang et al.*, 1996], volcanic injection of aerosols, interannual dynamical variability, and the impact of the export of dehydrated air to midlatitudes are not accounted for in this model study. The present model simulations also do not include the radiative-dynamical feedback explored by *Kiehl et al.* [1988] and *Mahlman et al.* [1994]. In the latter study, a cooling of approximately 8 K at 50 hPa was calculated near the pole in December during a 5-year experiment using the GFDL SKYHI model. This raises the possibility that enhanced PSC formation may occur in later years leading to a deeper ozone depletion. The GFDL model also revealed signs of altered stratospheric circulation in response to polar ozone decreases.

Inadequacies in horizontal and vertical resolution may also influence the results of this study. The ability of the model to effectively resolve the very sharp gradients associated with PSC-induced chemistry requires adequate horizontal resolution. The model does not precisely reproduce the breakdown of the southern polar vortex. This has implications on the rate of ozone dilution and makes a detailed comparison of observed trends with model calculations difficult.

Simulations are underway with an enhanced horizontal resolution (T32) version of the NASA Langley model. This new model also explicitly includes the feedback of the modeled ozone field on the radiative and dynamical calculations and improved tropospheric physical processes. We intend to report on these experiments when they are complete.

Acknowledgments. This research was performed with the support of the NASA Earth Observing System program. We are grateful to Ellis Remsberg and two anonymous reviewers for suggesting improvements to an earlier version of this manuscript.

References

- Atkinson, R. J., W. A. Matthews, P. A. Newman, and R. A. Plumb, Evidence of the mid-latitude impact of Antarctic ozone depletion, *Nature*, *340*, 290–294, 1989.
- Bojkov, R. D., C. S. Zerefos, D. S. Balis, I. C. Ziomas, and A. F. Bais, Record low total ozone during northern winters of 1992 and 1993, *Geophys. Res. Lett.*, *20*, 1351–1354, 1993.
- Brasseur, G., and S. Solomon, *Aeronomy of the Middle Atmosphere*, 441 pp., D. Reidel, Norwell, Mass., 1984.
- Cariolle, D., A. Lasserre-Bigorry, J.-F. Royer, and J.-F. Geleyn, A general circulation model simulation of the spring-time Antarctic ozone decrease and its impact on midlatitudes, *J. Geophys. Res.*, *95*, 1883–1898, 1990.
- Chandra, S., C. H. Jackman, A. R. Douglass, E. L. Fleming, and D. B. Considine, Chlorine-catalyzed destruction of ozone: Implications for ozone variability in the upper stratosphere, *Geophys. Res. Lett.*, *20*, 351–354, 1993.
- Chipperfield, M. P., and J. A. Pyle, Two-dimensional modelling of the Antarctic lower stratosphere, *Geophys. Res. Lett.*, *15*, 875–878, 1988.
- Douglass, A. R., R. B. Rood, J. A. Kaye, R. S. Stolarski, D. J. Allen, and E. M. Larson, The influence of polar heterogeneous processes on reactive chlorine at middle latitudes: Three-dimensional model implications, *Geophys. Res. Lett.*, *18*, 25–28, 1991.
- Eckman, R. S., R. E. Turner, W. T. Blackshear, T. D. A. Fairlie, and W. L. Grose, Some aspects of the interaction between chemical and dynamical processes relating to the Antarctic ozone hole, *Adv. Space Res.*, *13*, 311–319, 1993.
- Eckman, R. S., W. L. Grose, R. E. Turner, W. T. Blackshear, J. M. Russell III, L. Froidevaux, J. W. Waters, J. B. Kumer, and A. E. Roche, Stratospheric trace constituents simulated by a three-dimensional general circulation model: Comparison with UARS data, *J. Geophys. Res.*, *100*, 13,951–13,966, 1995.
- Fahey, D. W., et al., In situ measurements constraining the role of sulphate aerosols in mid-latitude ozone depletion, *Nature*, *363*, 509–514, 1993.
- Garcia, R. R., F. Stordal, S. Solomon, J. T. Kiehl, A new numerical model of the middle atmosphere, 1, Dynamics and transport of tropospheric source gases, *J. Geophys. Res.*, *97*, 12,967–12,991, 1992.
- Garcia, R. R., and S. Solomon, A new numerical model of the middle, 2, Ozone and related species, *J. Geophys. Res.*, *99*, 12,937–12,951, 1994.
- Granier, C., and G. Brasseur, Impact of heterogeneous chemistry on model predictions of ozone changes, *J. Geophys. Res.*, *97*, 18,015–18,033, 1992.
- Grose, W. L., J. E. Nealy, R. E. Turner, and W. T. Blackshear, Modeling the transport of chemically active constituents in the stratosphere, in *Transport Processes in the Middle Atmosphere*, pp. 229–250, edited by G. Visconti and R. Garcia, D. Reidel, Norwell, Mass., 1987.
- Grose, W. L., R. S. Eckman, R. E. Turner, and W. T. Blackshear, Antarctic ozone depletion and potential effects on the global ozone budget, in *Dynamics, Chemistry and Photochemistry in the Middle Atmosphere of the Southern Hemisphere*, edited by A. O'Neill and C. R. Mechoso, Kluwer Acad., Norwell, Mass., 1990.
- Hofmann, D. J., and S. Solomon, Ozone destruction through the heterogeneous chemistry following the eruption of El Chichón, *J. Geophys. Res.*, *94*, 5029–5041, 1989.
- Hofmann, D. J., et al., Ozone loss in the lower stratosphere over the United States in 1992–1993: Evidence for heterogeneous chemistry on the Pinatubo aerosol, *Geophys. Res. Lett.*, *21*, 65–68, 1994a.
- Hofmann, D. J., et al., Recovery of stratospheric ozone over the United States in the winter of 1993–1994, *Geophys. Res. Lett.*, *21*, 1779–1782, 1994b.
- Jiang, Y., Y. L. Yung, and R. W. Zurek, Decadal evolution of the Antarctic ozone hole, *J. Geophys. Res.*, *101*, 8985–8999, 1996.
- Kaye, J. A., A. R. Douglass, R. B. Rood, R. S. Stolarski, P. A. Newman, D. J. Allen, and E. M. Larson, Spatial and temporal variability of the extent of chemically processed stratospheric air, *Geophys. Res. Lett.*, *18*, 29–32, 1991.
- Kelly, K. K., et al., Dehydration in the lower Antarctic stratosphere during late winter and early spring, 1987, *J. Geophys. Res.*, *94*, 11,317–11,357, 1989.
- Kiehl, J. T., B. A. Boville, and B. P. Briegleb, Response of a general circulation model to a prescribed Antarctic ozone hole, *Nature*, *332*, 501–504, 1988.
- Mahlman, J. D., J. P. Pinto, and L. J. Umscheid, Transport, radiative, and dynamical effects of the Antarctic ozone hole: A GFDL “SKYHI” model experiment, *J. Atmos. Sci.*, *51*, 489–508, 1994.
- McCormick, M. P., R. E. Veiga, and W. P. Chu, Stratospheric ozone profile and total ozone trends derived from the SAGE I and SAGE II data, *Geophys. Res. Lett.*, *19*, 269–272, 1992.
- Newman, P. A., Comparison of modeled and measured total column ozone, in *The Atmospheric Effects of Stratospheric Aircraft*, Rep. of the 1992 Models and Measurements Workshop, pp. C1–C22, edited by M. J. Prather and E. E. Remsburg, NASA Ref. Publ. 1292, 1993.
- Prather, M., M. M. Garcia, R. Suozzo, and D. Rind, Global impact of the Antarctic ozone hole: Dynamical dilution with a three-dimensional chemical transport model, *J. Geophys. Res.*, *95*, 3449–3471, 1990.
- Prather, M., and A. H. Jaffe, Global impact of the Antarctic ozone hole: Chemical propagation, *J. Geophys. Res.*, *95*, 3473–3492, 1990.
- Rinsland, C. P., et al., Heterogeneous conversion of N₂O₅ to HNO₃ in the post-Mount Pinatubo eruption stratosphere, *J. Geophys. Res.*, *99*, 8213–8219, 1994.
- Roche, A. E., et al., Observations of lower-stratospheric ClONO₂, HNO₃, and aerosol by the UARS CLAES experiment between January 1992 and April 1993, *J. Atmos. Sci.*, *51*, 2877–2902, 1994.
- Santee, M., W. G. Read, J. W. Waters, L. Froidevaux, G. L. Manney, D. A. Flower, R. F. Jarnot, R. S. Harwood, and G. E. Peckham, Interhemispheric differences in polar stratospheric HNO₃, H₂O, ClO, and O₃, *Science*, *267*, 849–852, 1995.

- Solomon, S., R. W. Portmann, R. R. Garcia, L. W. Thomason, L. R. Poole, and M. P. McCormick, The role of aerosol trends and variability in anthropogenic ozone depletion at northern midlatitudes, *J. Geophys. Res.*, *101*, 6713–6727, 1996.
- Stolarski, R. S., P. Bloomfield, R. D. McPeters, and J. R. Herman, Total ozone trends deduced from Nimbus 7 TOMS data, *Geophys. Res. Lett.*, *18*, 1015–1018, 1991.
- Sze, N. D., M. K. W. Ko, D. K. Weisenstein, J. M. Rodriguez, R. S. Stolarski, and M. R. Schoeberl, Antarctic ozone hole: Possible implications for ozone trends in the southern hemisphere, *J. Geophys. Res.*, *94*, 11,521–11,528, 1989.
- Tuck, A. F., Synoptic and chemical evolution of the Antarctic vortex in late winter and early spring, 1987, *J. Geophys. Res.*, *94*, 11,687–11,737, 1989.
- Tuck, A. F., et al., Polar stratospheric cloud processed air and potential vorticity in the Northern Hemisphere lower stratosphere at mid-latitudes during winter, *J. Geophys. Res.*, *97*, 7883–7904, 1992.
- Turco, R. P., O. B. Toon, and P. Hamill, Heterogeneous physicochemistry of the polar ozone hole, *J. Geophys. Res.*, *94*, 16,493–16,510, 1989.
- Waters, J. W., L. Froidevaux, W. G. Read, G. L. Manney, L. S. Elson, D. A. Flower, R. F. Janot, and R. S. Harwood, Stratospheric ClO and ozone from the microwave limb sounder on the Upper Atmosphere Research Satellite, *Nature*, *362*, 597–602, 1993.
- Waugh, D. W., et al., Transport of material out of the stratospheric Arctic vortex by Rossby wave breaking, *J. Geophys. Res.*, *99*, 1071–1088, 1994.
- World Meteorological Organization (WMO), Report of the International Ozone Trends Panel 1988, *WMO Rep. 18*, World Meteorol. Organ., Geneva, 1989.
- World Meteorological Organization (WMO), Scientific assessment of ozone depletion: 1991, *WMO Rep. 25*, World Meteorol. Organ., Geneva, 1992.
- World Meteorological Organization (WMO), Scientific assessment of ozone depletion: 1994, *WMO Rep. 37*, World Meteorol. Organ., Geneva, 1995.

W. T. Blackshear, R. S. Eckman, W. L. Grose, and R. E. Turner, NASA Langley Research Center, Mail Stop 401B, Hampton, VA 23681. (e-mail: r.s.eckman@larc.nasa.gov; grose@haloe.larc.nasa.gov; r.e.turner@larc.nasa.gov)

December 6, 1995; revised May 30, 1996; accepted June 28, 1996.

Figure 1. Decadal trends in annually averaged total ozone derived from TOMS, SBUV, and ground-based Dobson ozone from January 1979 to May 1991. Adapted from *WMO* [1995], Figure 1-7.

Figure 2. Vertical profiles of percentage difference in zonally averaged ozone mixing ratio for April, July, October, and January between the simulation with PSC chemistry (case B in text) and the no PSC simulation at 80°S (left side) and 36°S (right side) during the first through second (dotted lines) and second through third (solid lines) model years. Positive numbers represent ozone decreases.

Figure 3. Vertical profiles of zonally averaged HNO₃ mixing ratio (parts per billion by volume) for April, July, October, and January during the second year for the simulation with PSC chemistry (case B in text, solid line) and the no PSC simulation (dotted line) for 80°S (left side) and 36°S (right side).

Figure 4. (a) Globally integrated ozone in Dobson Units for the baseline (no PSC) simulation (solid line) and for case B simulation (dotted line). (b) Percent difference in globally integrated ozone between case B and no PSC simulation.

Figure 5. (a) As in Figure 4b except for southern hemisphere only. (b) As in Figure 4b except for northern hemisphere only.

Figure 6. Zonally averaged vertical profile of HNO₃ mixing ratio in January at 80°S for each year of the model simulation for case B.

Plate 1. Seasonal evolution of model-calculated zonally averaged, column-integrated ozone (Dobson Units) for April, July, October, and January during the second year of the case B simulation.

Plate 2. As in Plate 1, except for HNO_3 mixing ratio (parts per billion by volume) at 45 hPa.

Plate 3. As in Plate 1, except for Cl_x mixing ratio (parts per billion by volume) at 45 hPa.

Plate 4. Percent difference in column integrated, zonally averaged ozone between the simulation with PSC chemistry (case B in text) and the no PSC simulation. Negative numbers represent ozone decreases.

Plate 5. As in Plate 4 except for case A with enhanced level of denitrification.

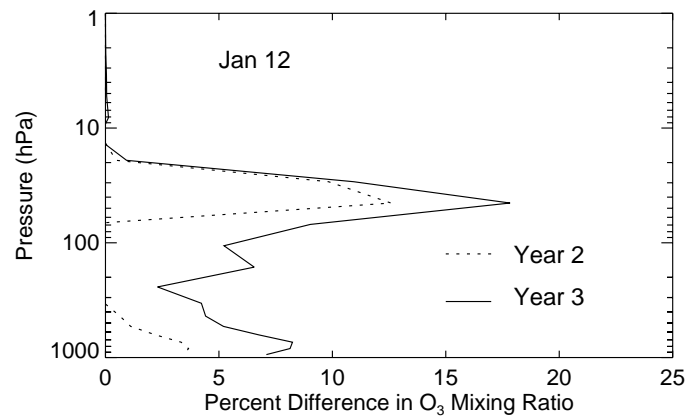
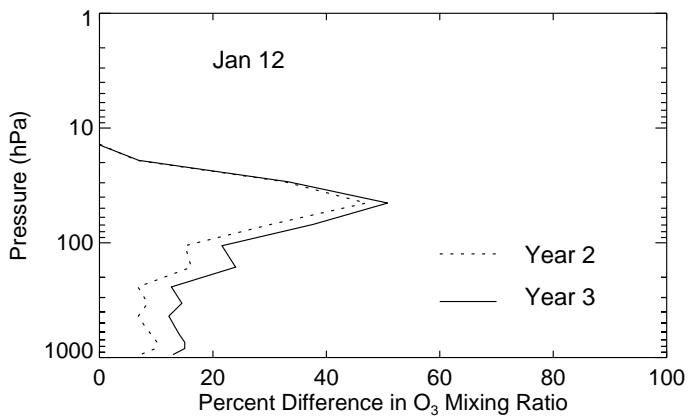
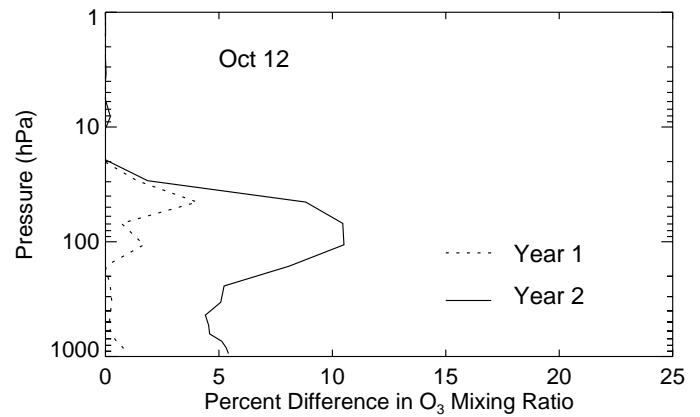
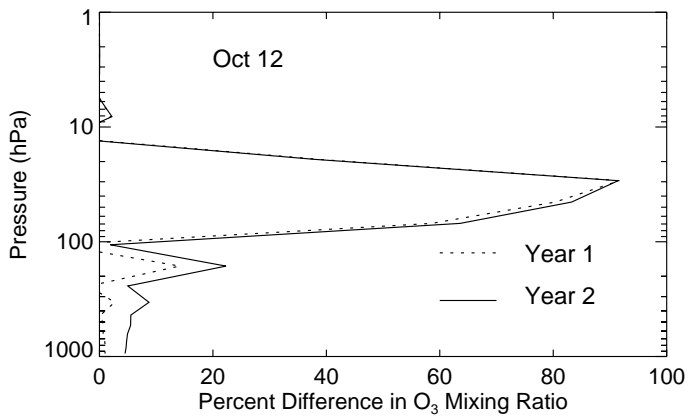
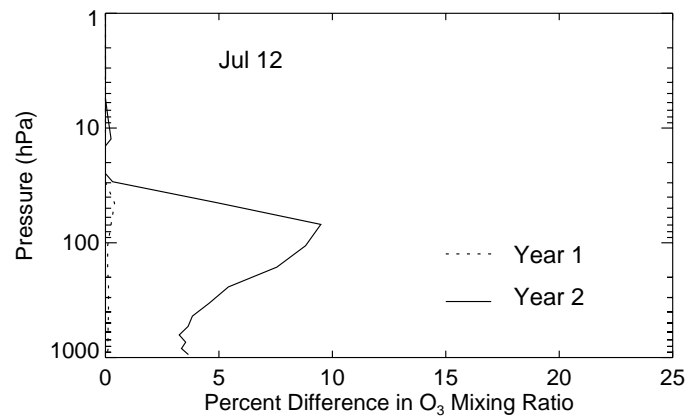
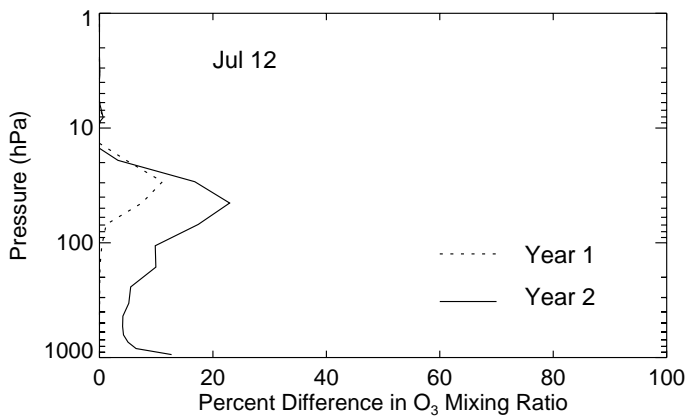
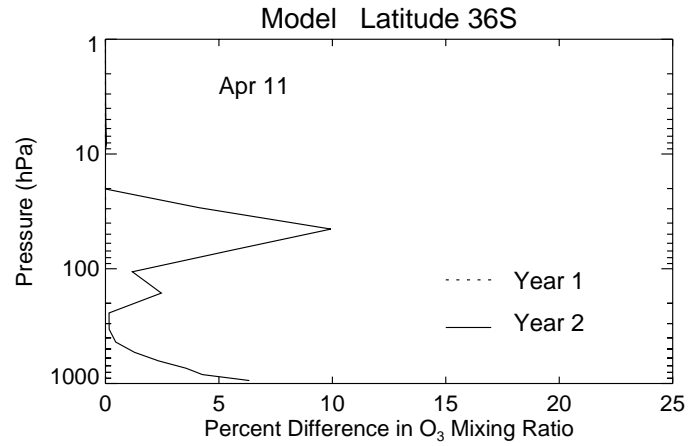
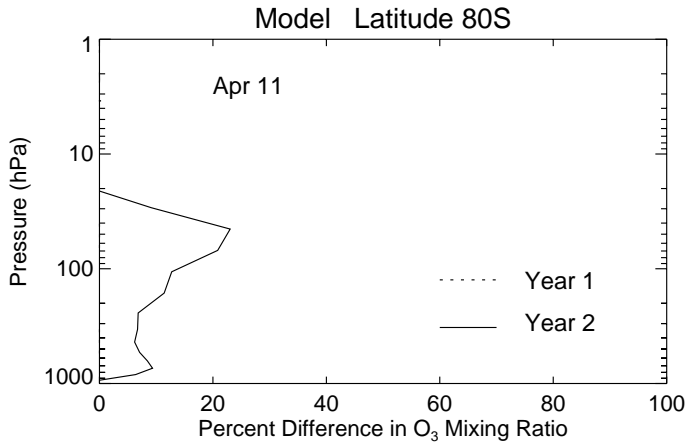


Figure 2

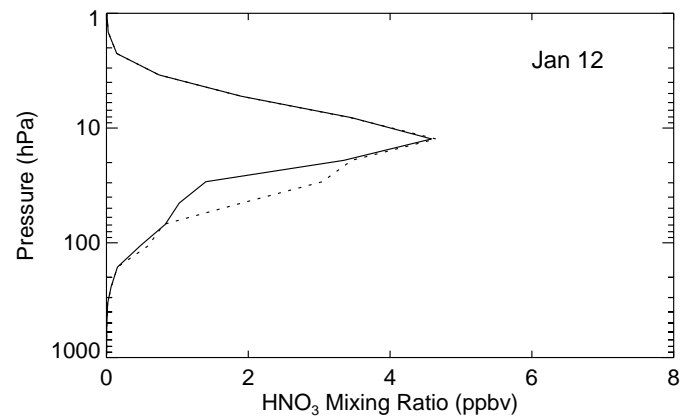
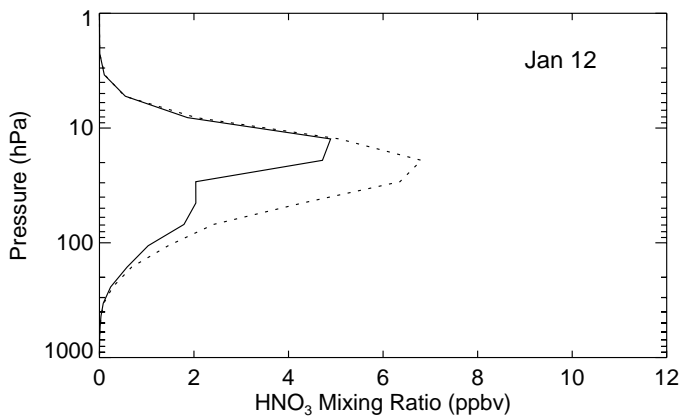
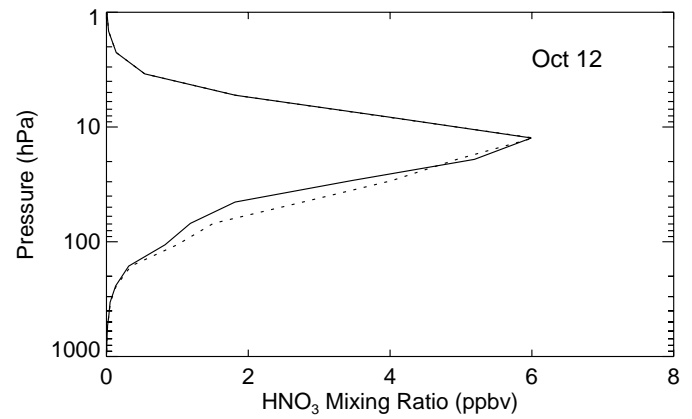
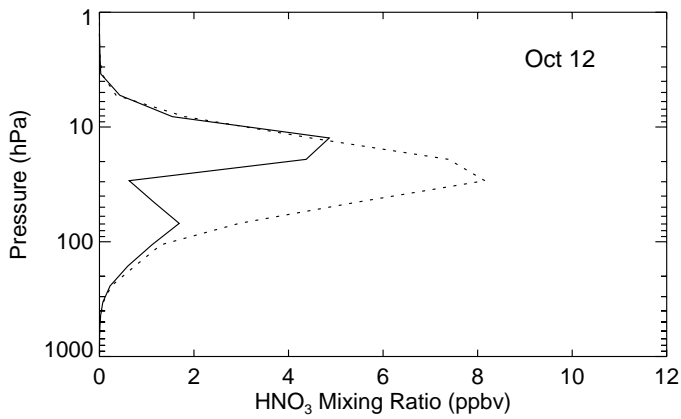
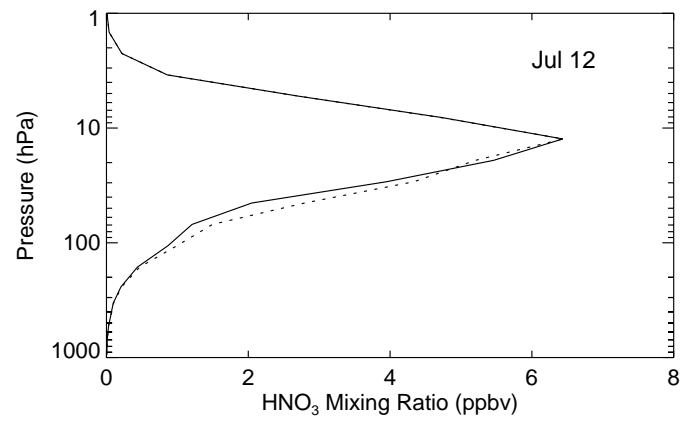
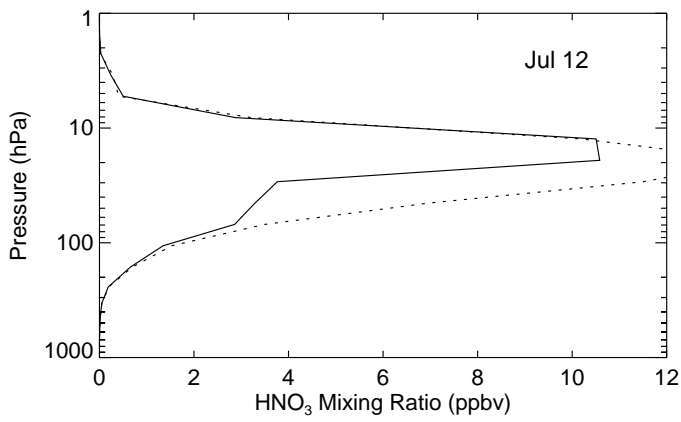
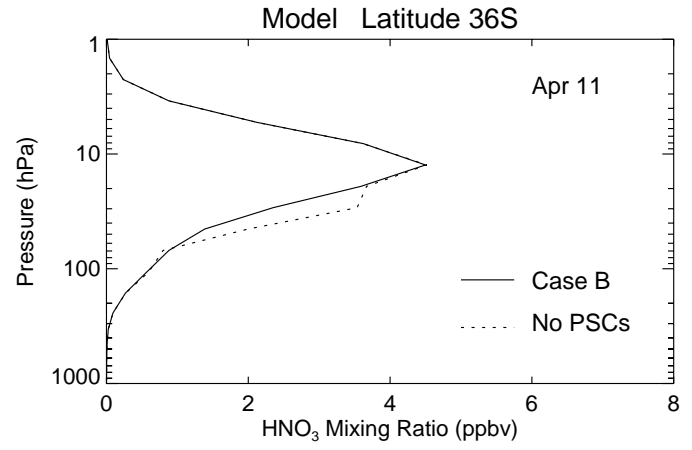
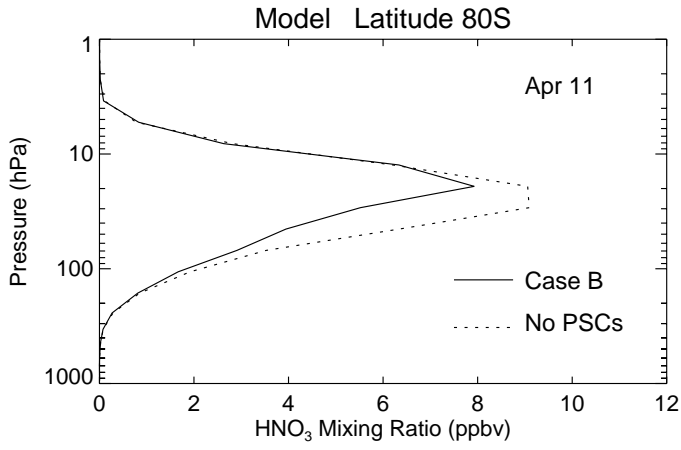


Figure 3

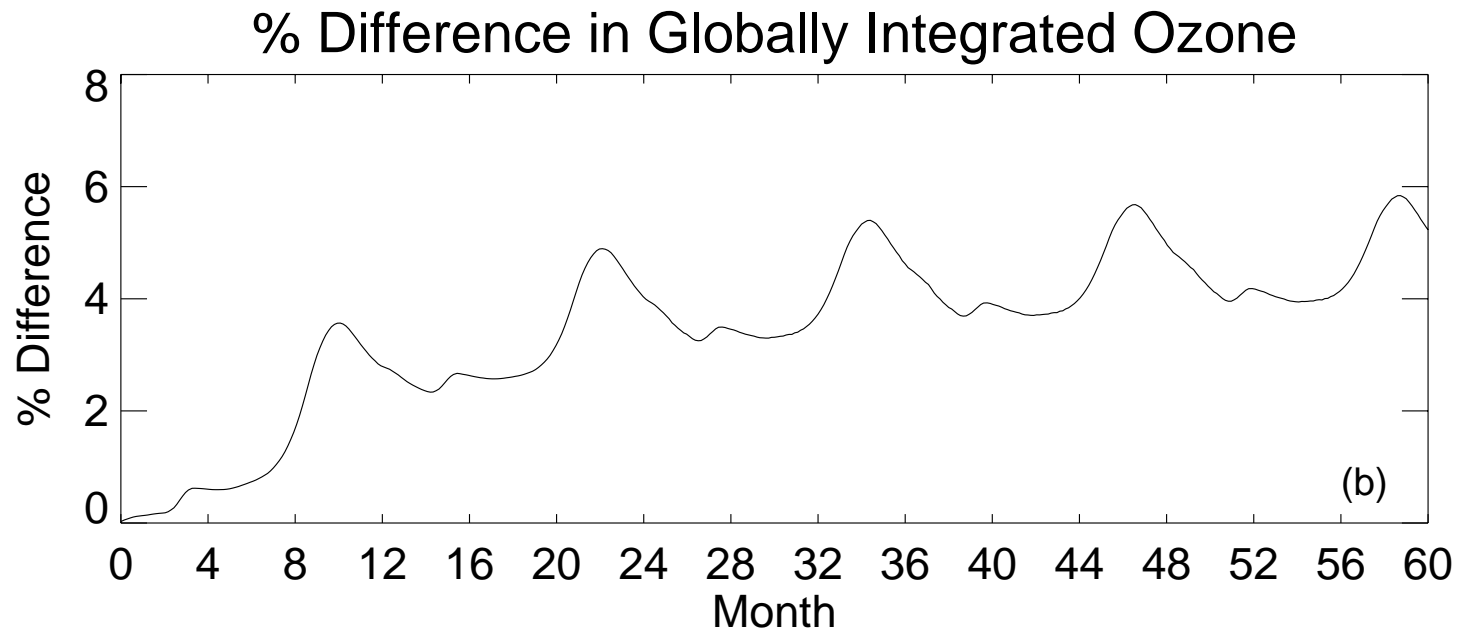
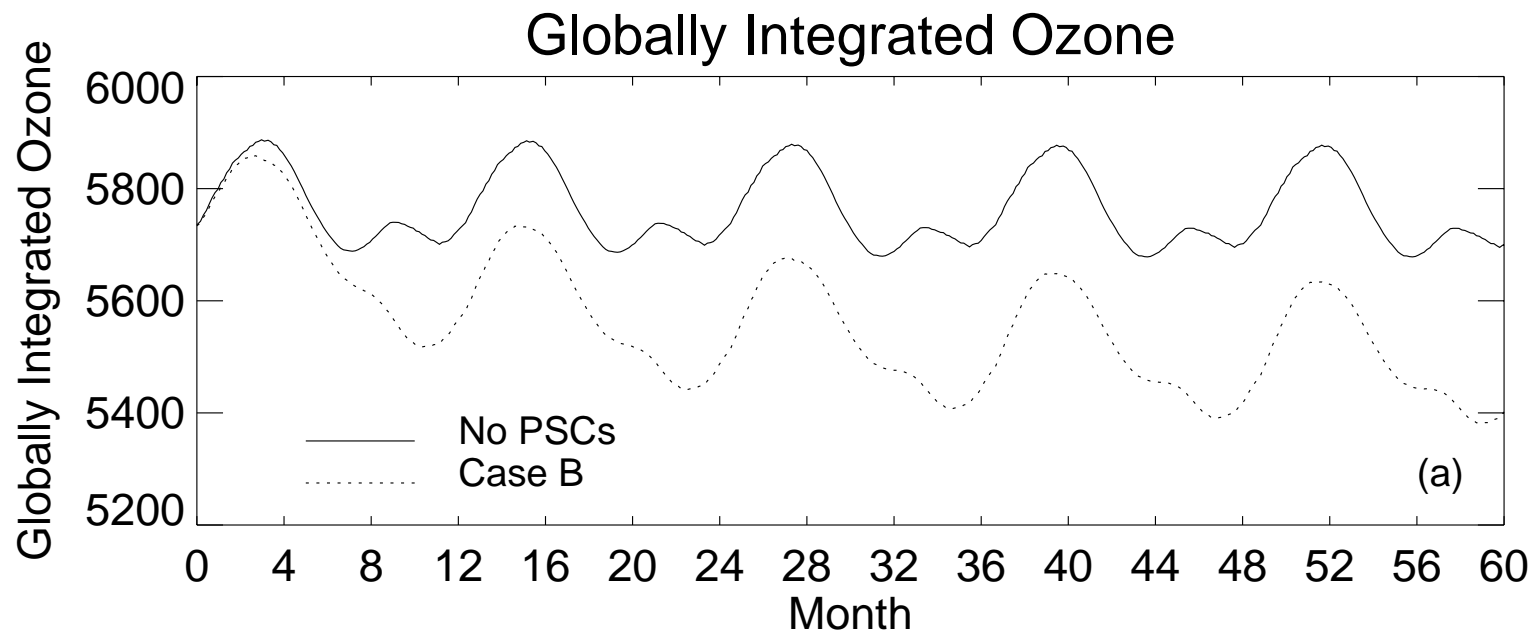


Figure 4

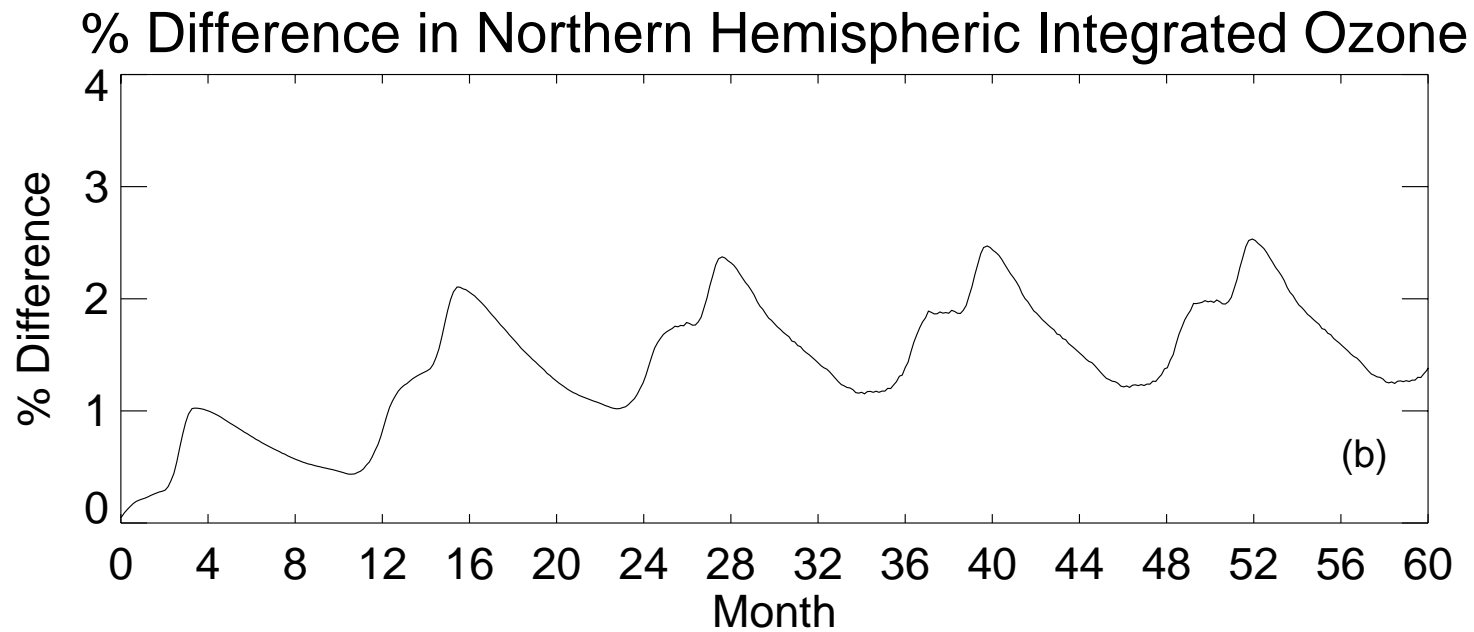
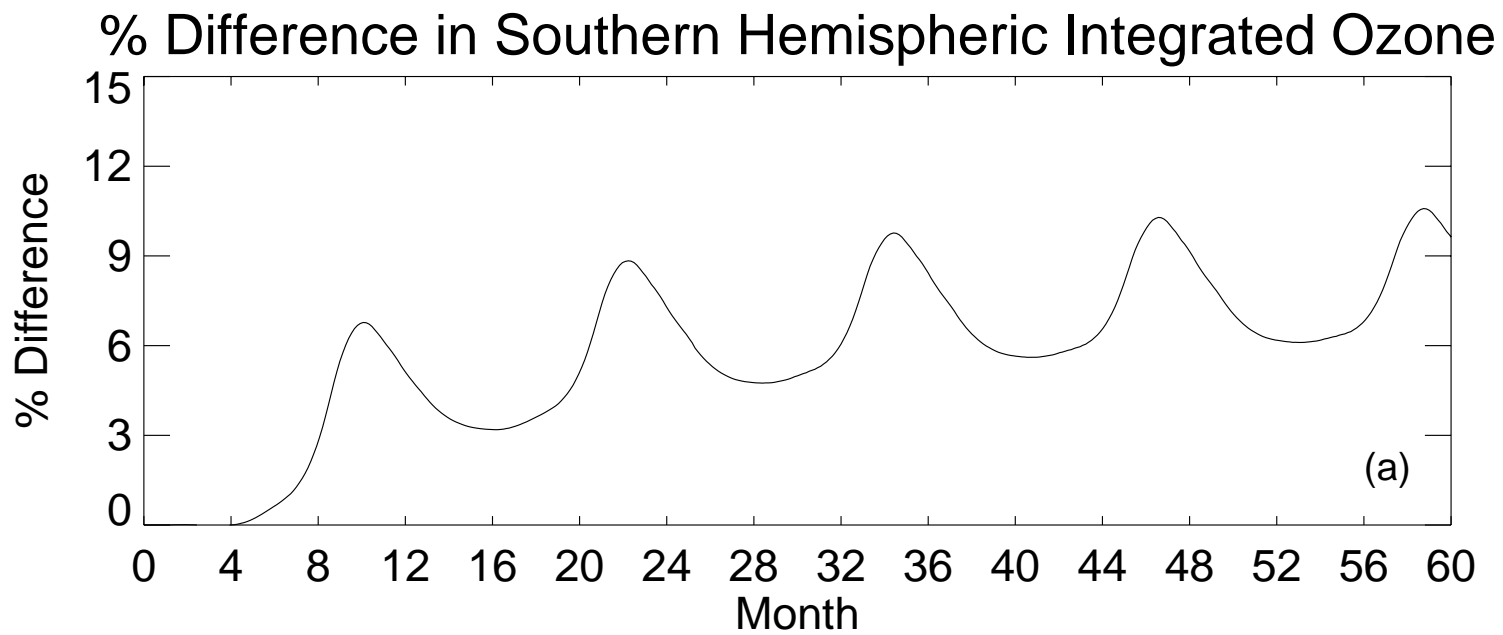


Figure 5

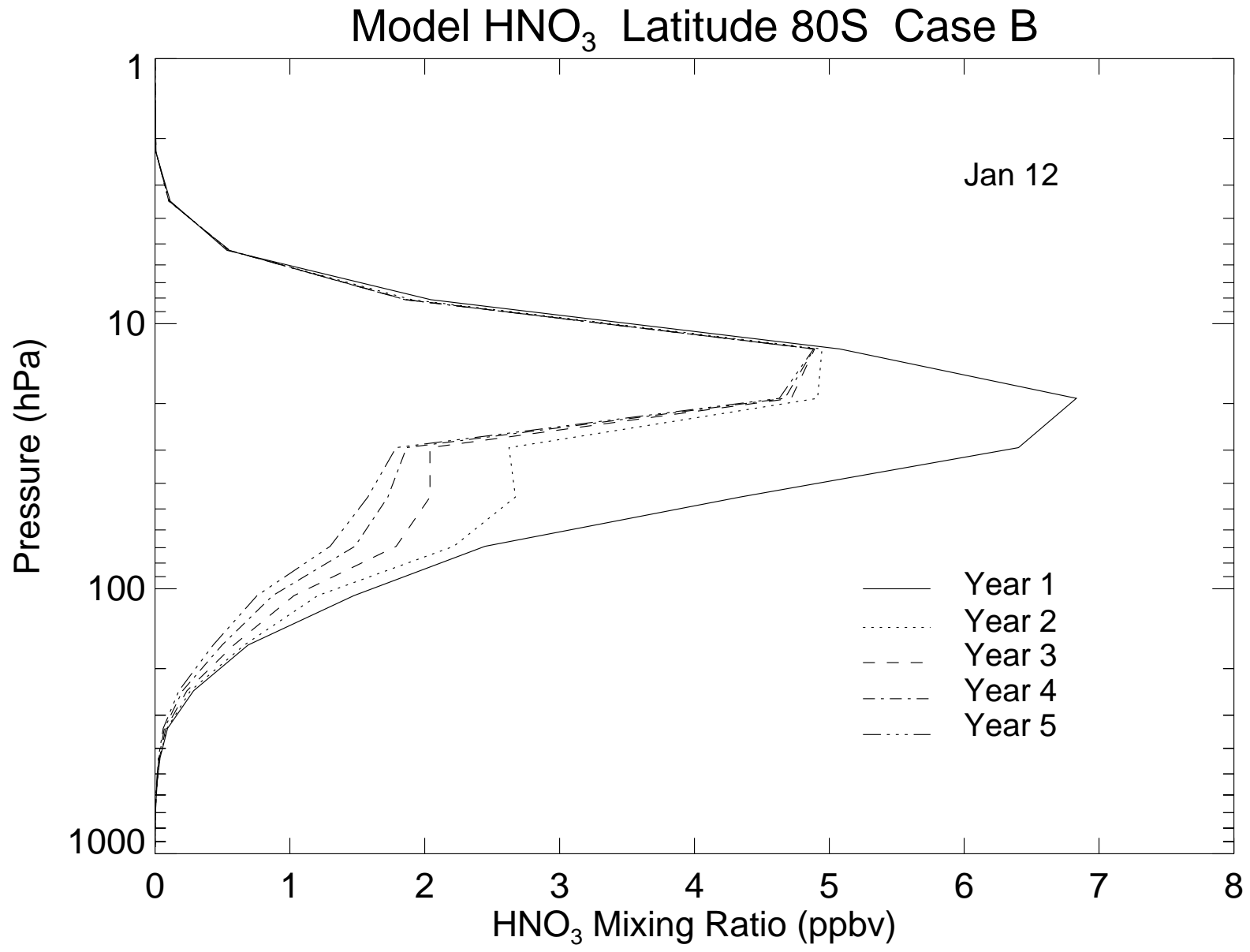
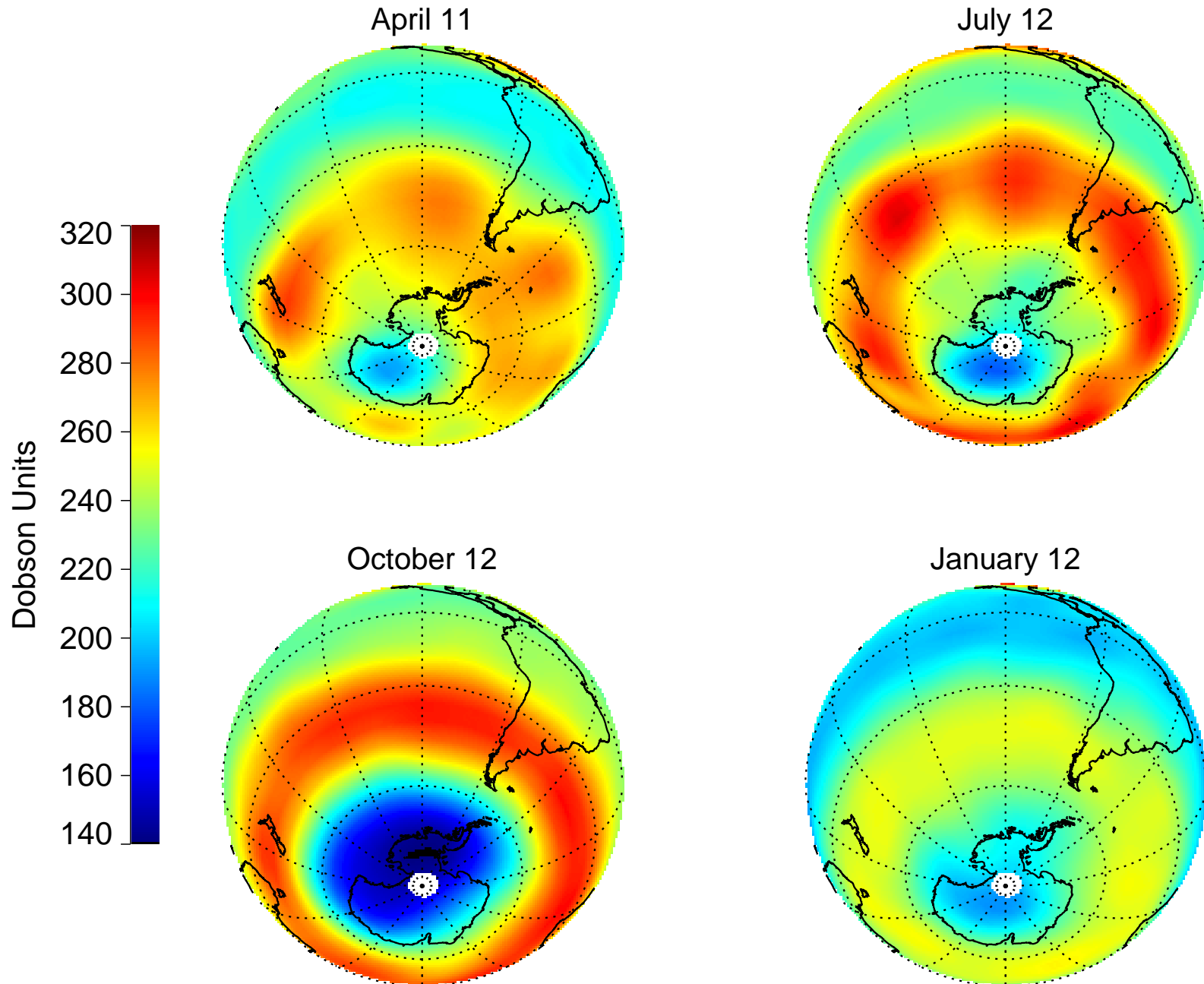
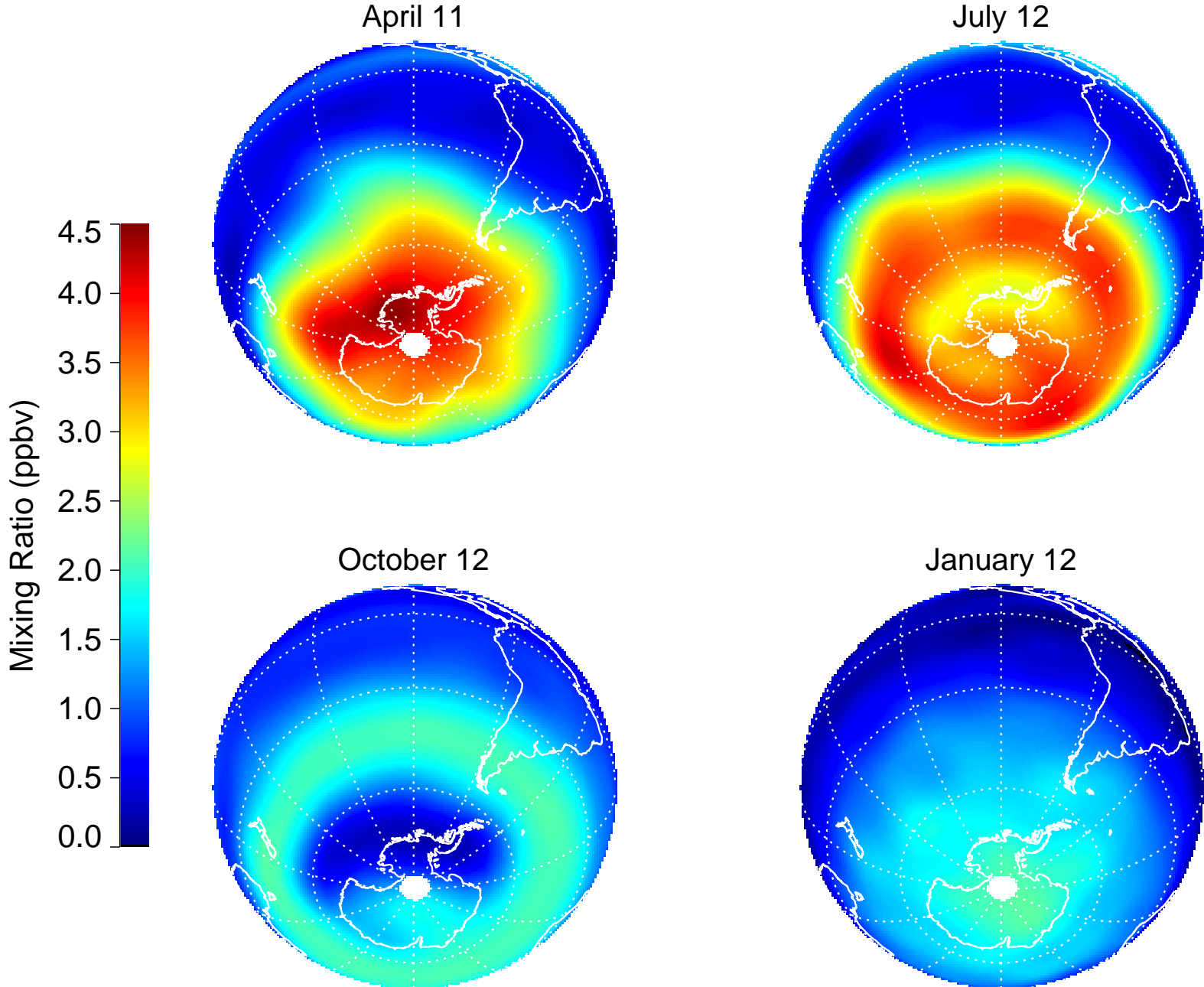


Figure 6

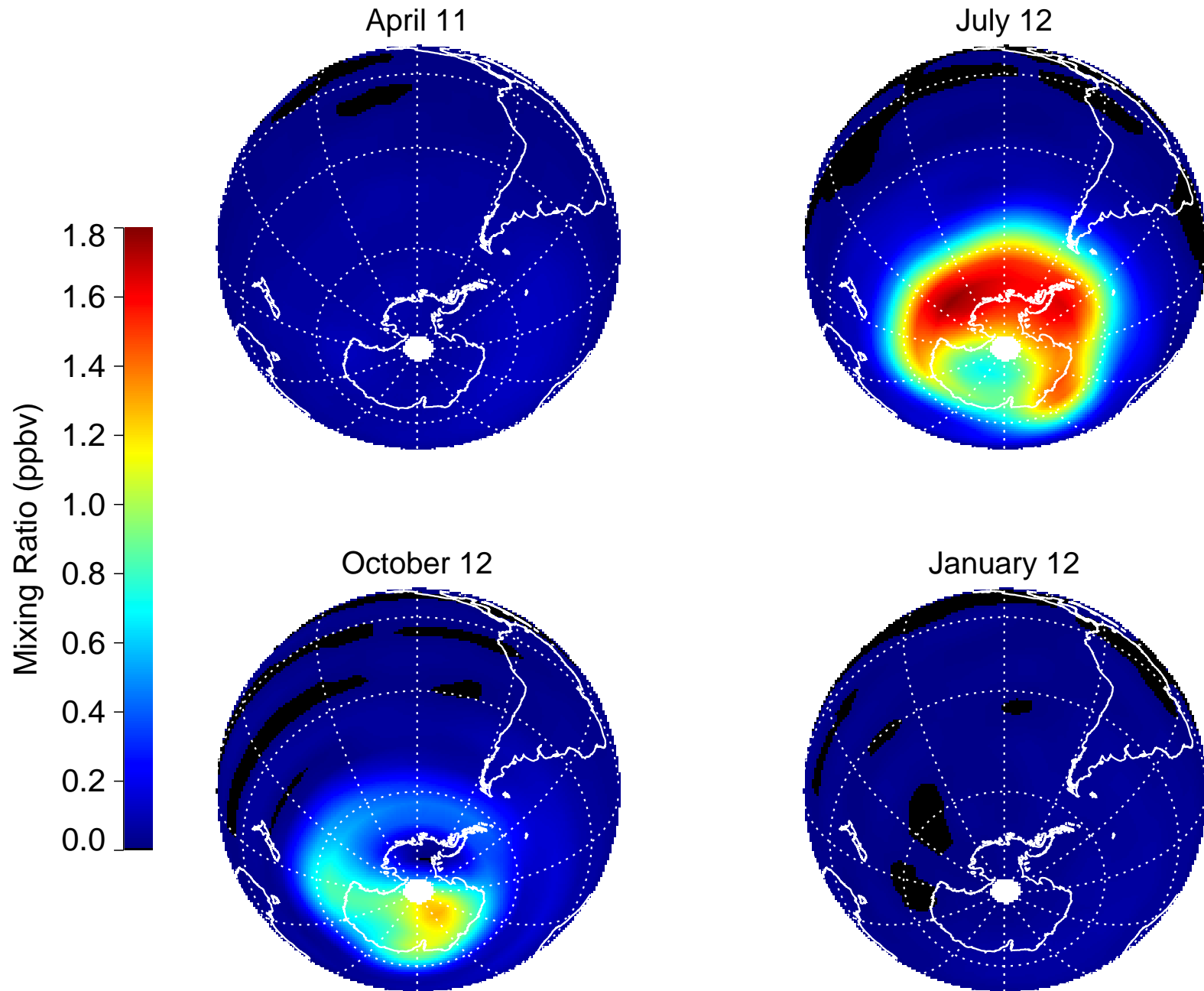
3-D Model O₃ Column



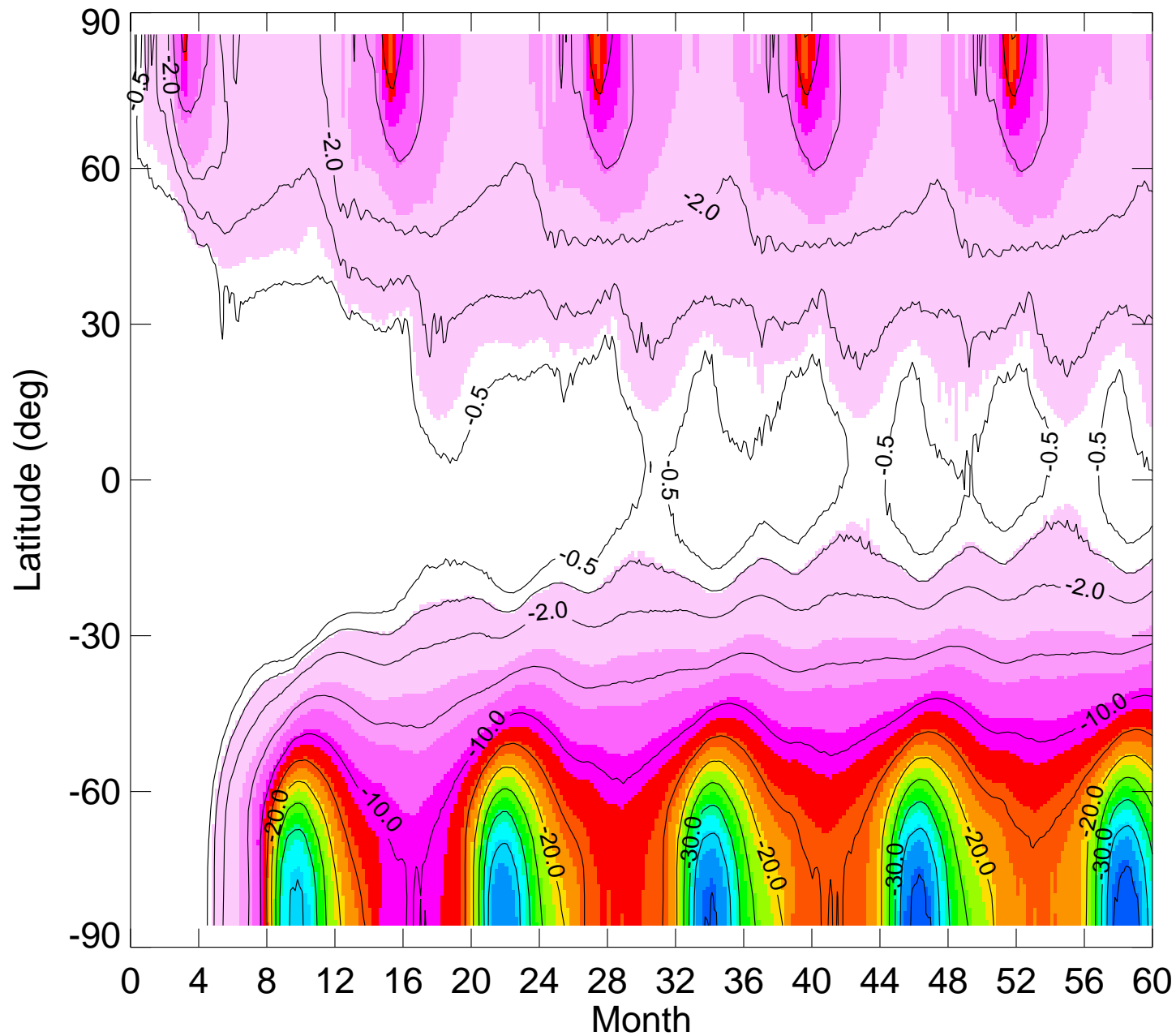
3-D Model HNO₃ 45 mb



3-D Model Cl_x 45 mb



% Difference in Total Ozone Case B / No PSC



% Difference in Total Ozone Case A / No PSC

